



Robotic construction of a self-balancing glass masonry vault: DEM study of stability during the construction stages

Vittorio PARIS^{a*}, Nicola LEPORE^b, Edvard P.G. BRUUN^c,
Giuseppe RUSCICA^a, Mario Daniele Piccioni^b, Alessandro BEGHINI^d, Stefana PARASCHO^c, Sigrid
ADRIAENSSENS^c,

* University of Bergamo, Italy
vittorio.paris@unibg.it

^a University of Bergamo, Italy

^b Polytechnic University of Bari, Italy

^c Princeton University, USA

^d SOM | Skidmore, Owings & Merrill LLP

Abstract

Self-balancing construction technologies were used for centuries in the building of masonry domes and vaults. Such construction techniques were made possible through the careful design of the block tessellation and the structural form, which enabled construction of complex geometries that remain stable without falsework. These historical masonry technologies have a disruptive potential for today's construction industry when coupled with emerging innovations such as novel computational form-finding approaches and robotic fabrication. This paper presents a structural analysis of the construction stages for a doubly curved, compression-only, 2-meter-tall masonry vault inspired by traditional construction technologies and built with a cooperative human-robot fabrication process. Two ABB-IRB 6400 industrial robotic arms were precisely sequenced to alternate placing a masonry block and providing temporary support to the unfinished structure. As a result, no form- or falsework was needed during any construction stage. The paper reports an iterative procedure based on the Limit State Analysis (LSA) and Discrete Element Method (DEM) to numerically study the equilibrium of the masonry vault during all construction stages.

Keywords: Shell, Vault, Masonry, Robotic Construction, Discrete Element Model, Limit State Analysis, Self-balancing

1. Introduction

Ancient master builders have built arches, vaults, and domes using masonry for millennia. These ancient forms create impressive architectural spaces that in some cases surpass the longevity of contemporary structures [1]. From the 2nd millennia BCE onwards, self-balancing construction techniques have been in use to realize many such complex structures [2]. The pitched vault [3] is perhaps the first self-balancing building system developed, which dates back to as early as the 21st century BCE [4] and is still applied in a few parts of North Africa [5]. As shown by various studies [3] [6] [7], the self-balanced state under construction is due to several factors all related with the construction work such as: the properties of building materials [6], the orientation of bed joints (as shown in figure 1) [3], and the tessellation [7].

Considering all of these factors, through history, several self-balancing construction technologies have also been developed [7] [8] [9], even the ones built in dry-stone masonry, widespread in the vernacular architecture of all the Mediterranean area [10]. Among all, the herringbone [11] and tile vaulting [12] constitute the most influential systems [9]. Santa Maria del Fiore's dome in Florence (1418-1436) [13] represents a notable example of the herringbone technique applied on a large scale.

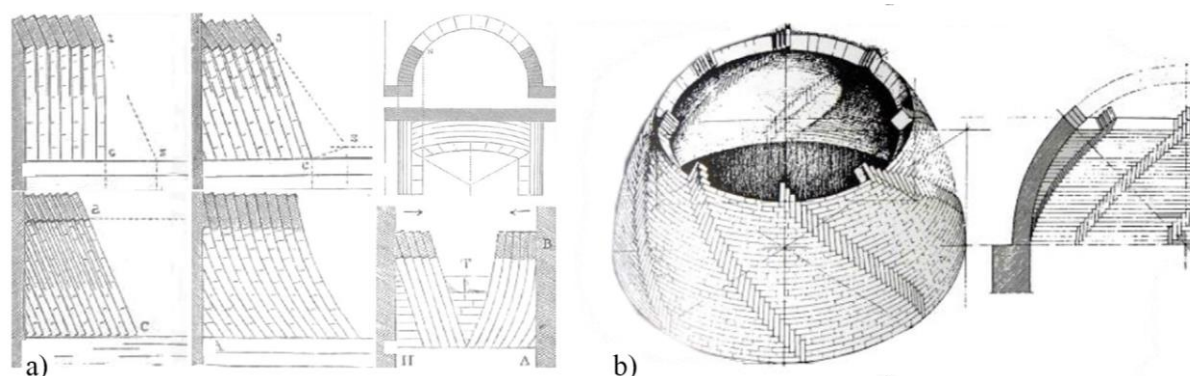


Figure 1. a) The pitched vaulting technique, different scheme to lay bricks. Drawing of A. Choisy [14]. b) Revolution dome and herringbone spiralling tessellation. Drawing of F. Gurrieri [15].

As illustrated in figure 1b), the herringbone technique gets its name from its characteristic tessellation pattern: the bricks are arranged in an alternating horizontal and vertical manner [16]. Due to this tessellation and a precise sequence of laying bricks, self-supporting structural actions are formed in the dome even during its construction [17]. On the other hand, tile vaulting methods, originating in Spain around the 13rd-14th century CE [12], allows the construction of doubly-curved structures without the aid of any temporary supports through the use of fast setting gypsum mortar coupled with light tiles [18]. This technique has been a topic of recent research [6] [19] since its application to the construction of form-found vault geometries is more manageable than other self-balanced technologies. Despite specific differences in geography or time period, all the historic self-balancing masonry construction techniques mentioned share an important choice of laying sequence and structural form the technique is being applied to. The potential of these historic technologies in the construction of complex geometries without falsework is being increasingly rediscovered in the context of emerging innovations such as novel computational form-finding approaches and robotic construction technologies.

Different approaches have been developed from the structural point of view to analyse masonry curved structures. A significant milestone toward understanding the structural behaviour of voussoir arches and vaults was made by Heyman [20], who reinterpreted the geometrical and equilibrium-based rules used by the ancient master builders through the Limit State Analysis (LSA) framework, reclaiming the power of graphic static (GS) approaches [21]. The success of this approach was due to the possibility of obtaining an accurate estimation of collapse loads using a straightforward constitutive model known as the no-tension model [22]. This model does not require the calibration of any parameters for the masonry's mechanical characterisation, which overcomes the high level of uncertainty that is usually associated with masonry structures, especially in historical constructions. More recent LSA methods based on the Thrust Line Analysis (TLA), have further reworked and extended to the analysis of complex three-dimensional structures [23] [24] [25]. In these approaches, the search for a thrust line entirely contained within the vault's thickness was extended to the three-dimensional space, as a search for discrete compression-only network or continuum unilateral membrane. Thus, according to the Safe Theorem [21], the masonry structure is stable if the thrust network [26] or surface [27] lies entirely between the intrados and the extrados surface of the vault. From a numerical point of view, literature [28] [29] [30] shows that Discrete Element Modelling (DEM) is particularly suitable to analyse the

equilibrium of masonry structures. Indeed, Lemos and other researchers have proven its validity to simulate the static and dynamic behaviour of masonry structures [28] [31]. Although the potential of the methods mentioned above to analyse complete structures is well known, evaluating the equilibrium of masonry structures under construction is scarcely explored; few works that address this, are presented in the literature [17] [32].

This paper extends the existing literature on the structural analysis of masonry structures by applying LSA and DEM methods to calculate the structural performance of a doubly-curved compression-only glass brick shell during its construction stages. The main challenge is how to investigate the vault's structural behaviour in each construction stage, while also accounting for the fact that the entire building process is carried out through a human-robot fabrication process without temporary form-or-falsework. To perform this analysis, an iterative procedure was developed that accounts for the action of the robotic arms on the structure under construction.

This research culminated in the robotic fabrication of a full-scale vault prototype at the “Anatomy of Structure” exhibit hosted at the Ambika P3 Gallery in London [33], and shown in figure 2. Different aspects of this research, from the development of the cooperative robotic fabrication strategy to the analysis of different construction sequences, are further detailed in recent works [33] [34] [35] [36].

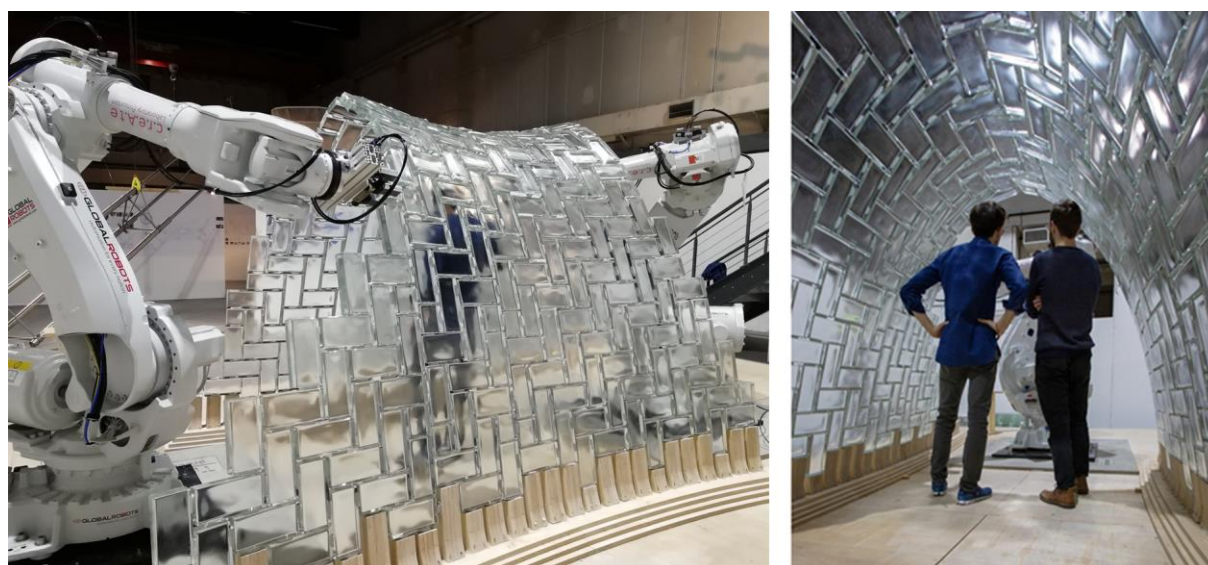


Figure 2. Robotic fabrication of a masonry vault for the “Anatomy of Structure” exhibit.

The paper is organised as follows: section 2 describes the geometry of the vault and the material system; section 3 provides an overview on the construction process adopted and illustrates the analogies with historical self-balancing technologies; section 4 describes the methodology adopted to assess the structural state of the vault during its construction; section 5 presents the structural analysis conducted and the results; and section 6 concludes the paper and presents a discussion.

2. Vault geometry and material

The motivation for the current research comes from the exploration of ultra-light, yet efficient and strong, timber vault structures. This work was inspired by historical construction methods that relied on inclined courses to build vaults with the aid of only light falsework [37]. Starting from this idea, the current project was then developed with the goal of building a geometrically complex self-balancing shell without the aid of any temporary falsework. To achieve this goal, industrial robotic arms were used to both place bricks in precise complex spatial orientations and to act as temporary support to the unfinished structure [34]. As shown in figure 3, the vault has a form-found geometry, characterised by

a saddle shape with a catenary profile. The span of the vault is 2.7 meters, with a length of 4.4 meters, and a rise about 2.2 meters on the outside edges and 1.9 meters for the central arch. Glass bricks were the primary elements used for the structure. As is common in masonry constructions, the geometry of the vault had to be defined so as to minimise any tensile forces. A form-finding approach, based on the Airy's stress function [38], enabled the calculation of a doubly-curved compression-only shell. The geometry was found by an iterative process, which took into account the real distribution of the self-weight of the structure [39].

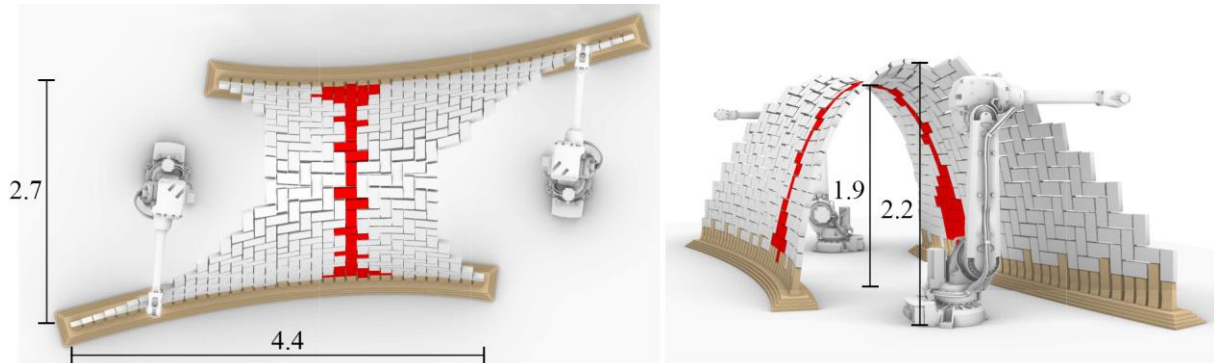


Figure 3. Geometry of the form-found shell. The central arch (red) corresponds to the first portion of the vault built. The two sides of the vault (white) are built only after completing the central arch.

Using standardised glass bricks, simplified construction by avoiding the need to field cut complex brick shapes to resolve unique geometric conditions. The material used in the joints needed to be fast-setting, rigid and with enough strength to hold the brick in place as it was placed. As reported in [34], this material was also used to compensate for the gap between different bricks courses and to deal with construction tolerances. For all these reasons, fast-setting epoxy putty [40] was selected as the joint mortar.

3. The construction phases

Two robotic arms (ABB-IRB 6400) were used to build the vault. A combination of historical technologies, such as herringbone and pitched techniques, allowed for the design of a precise construction process, with two distinct phases [34]. Phase **I** consists of all the construction stages related to the central arch, which was the first portion of the structure to be built. The central arch's construction is started from one side of the vault and bricks are then laid sequentially until the opposite side of the vault has been reached. The process of developing a robotic fabrication sequence that maintains stability during the construction is discussed in detail in recent works [34] [36]. Phase **I** ends when the last brick at the base of the arch is laid, this specific construction stage is denoted in this paper as **I-h**. Phase **II** follows phase **I**; here, the robot builds outward from the central arch to complete the remaining portion of the vault.

These two phases are characterised by the manner in which the two robotic arms were used. During phase **I**, the robots work cooperatively to build the central arch, one supports the incomplete arch while the second places the new glass brick. In phase **II**, the two robotic arms work separately, building two different portions of the vault; these portions are shown as the white bricks in figure 3.

This construction process incorporates several characteristics of the historical self-balancing technologies discussed in the introduction. In phase **I**, similar to the tile vaulting technique, the fast-setting property of the epoxy allows the glass bricks to maintain their position as they are laid. Meanwhile in phase **II**, the vault's tessellation is similar to the traditional herringbone technique, linking together two consecutive brick courses. Finally, the overall construction sequence is inspired by the pitched vault technology, where several consecutive self-balancing substructures are created before the

full structure is completed. These substructures are shown in figure 4, where in each construction stage, **II-a**, **II-b**, **II-c**, a new arch is built.

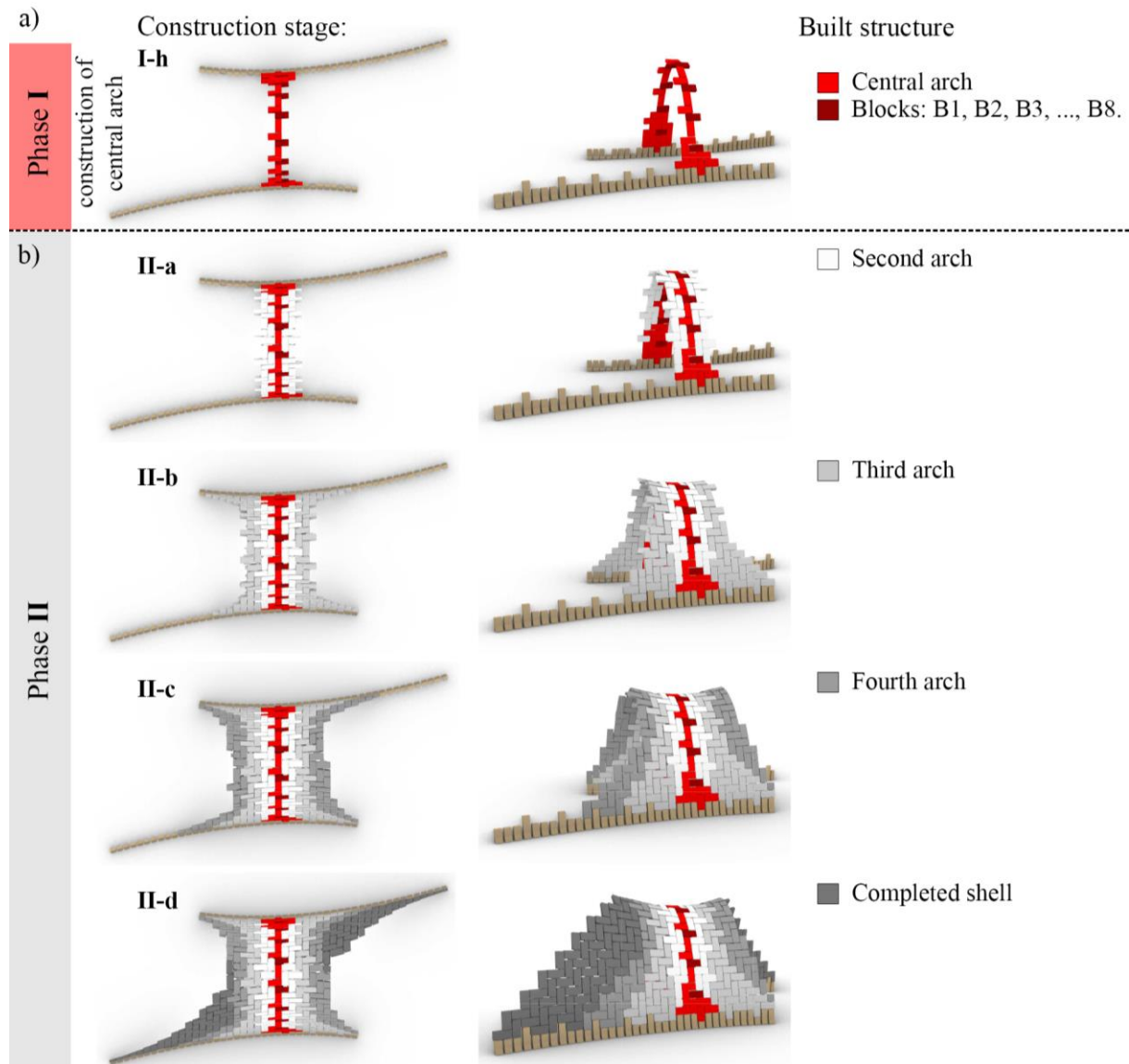


Figure 4. Construction process for the masonry vault.. a) Final stage of phase **I** and the closing of the central arch (construction stage **I-h**). b) phase **II**, where each stage is defined by the construction of a new inclined arch substructure.

4. Methodology for structural analysis

An evaluation of phase **I** was performed to assess the balanced state during construction. First a detailed TLA was carried out, dividing the central arch into individual blocks equivalent to the number of glass bricks. Thus, the equilibrium of the full structure was investigated by simulating the sequential placement of the bricks. As a result, for each construction stage related to phase **I**, an estimation of the external forces required to achieve stability was determined. These forces represent the static interaction between the structure and the robotic arms. According to LSA, no-tension material (i.e., any tensile

strength provided by the epoxy putty is neglected) is adopted to perform TLA, therefore this analysis is a conservative investigation.

The epoxy putty's realistic material properties were considered in a detailed numerical analysis conducted by DEM, which was carried out for both phases in order to investigate the balanced state and to estimate the displacements associated with each construction stage. The vault was modelled in the commercially available DEM software, 3DEC (Itasca, Minneapolis, MN, USA) [41], which allows to analyse masonry structures as a complex system of blocks [28]. These blocks can slide along their interfaces, collide or even detach [29] [30]. Through the explicit integration of Newton's laws of motion, using the finite-difference method and assuming small time-steps, the algorithm permits the evaluation of the structural behaviour of a system of bodies (either deformable or rigid) subjected to static or dynamic loads.

In the analyses performed, the vault's bricks are modelled as rigid blocks, whose size corresponds to that of the actual glass brick, which is then attached to a layer of epoxy putty surrounding it. Adopting this discretisation, the system of rigid bodies represents a good approximation of the form-found shell's structural behaviour, since the deformation is lumped at the joints. The material properties of the epoxy putty are used to model the interfaces, where a Mohr-Coulomb model with a tensile cut-off is assumed. As illustrated in figure 5, this nonlinear interface behaviour is ruled by the joint parameters: JK_n , JK_s , J_{ten} , J_{fric} and J_{coh} [42]. The JK_n , JK_s terms represent the normal and the shear stiffness of the rigid body's interfaces, respectively, while J_{ten} is the tensile strength, J_{fric} is the friction angle, and J_{coh} is the cohesive capacity. These parameters are determined based on the epoxy material's specifications [40] and verified by experiment tests, incorporating a safety coefficient.

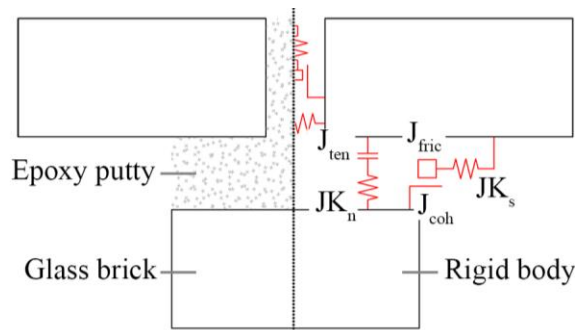


Figure 5. Joint parameters for the rigid bodies interface (adapted from [43]).

5. Analysis and results

Both phases of construction for the masonry vault were analysed, with the purpose of verifying the self-balancing state during the different stages. Sections, 5.1 (phase **I**) and 5.2 (phase **II**) describe the structural behaviour of the partially completed structure throughout the construction: arch behaviour is expected in phase **I**, and a compression-only shell behaviour in phase **II**

5.1 Phase **I**

As mentioned in section 4, TLA is executed to assess the equilibrium state of the central arch and determine the external forces that the robots must apply to guarantee this state of equilibrium. Therefore, all TLA were performed assuming that the robotic arms act as a support to the arch during construction. Although the final form-found shell was designed to achieve a fully-compressed membrane stress state, it was found that during construction the initial central arch was unable to achieve optimal structural behaviour. This is shown in figure 6a: the thrust line (red) of the central arch under construction does not entirely lie in the cross-section of initial form-found shell geometry. For this reason, the form of the complete shell had to be re-designed to ensure stability during construction.

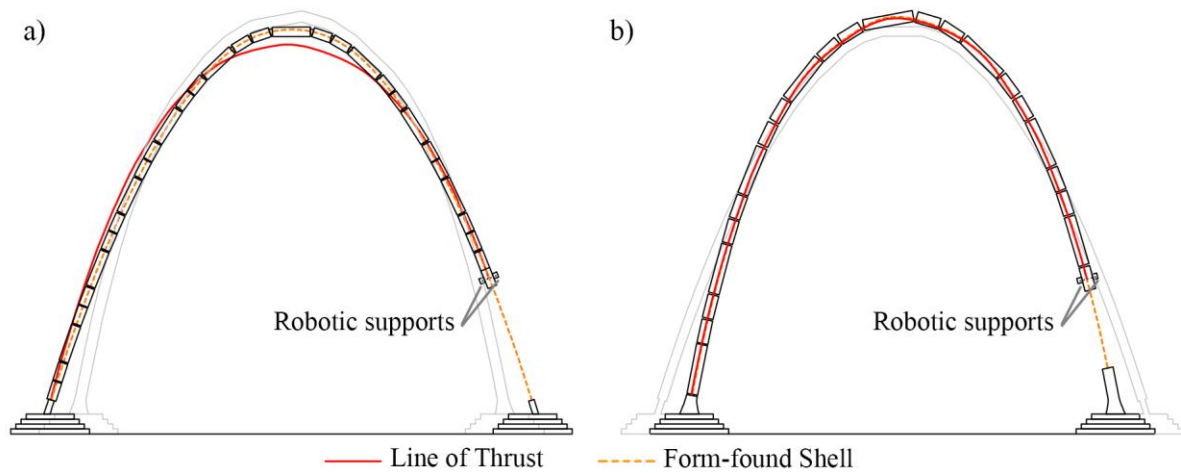


Figure 6. TLA for central arch under construction. a) the thrust line (red) of the arch under construction falls outside of the midline of the shell geometry. b) the thrust line (red) and midline of the re-designed arch coincide

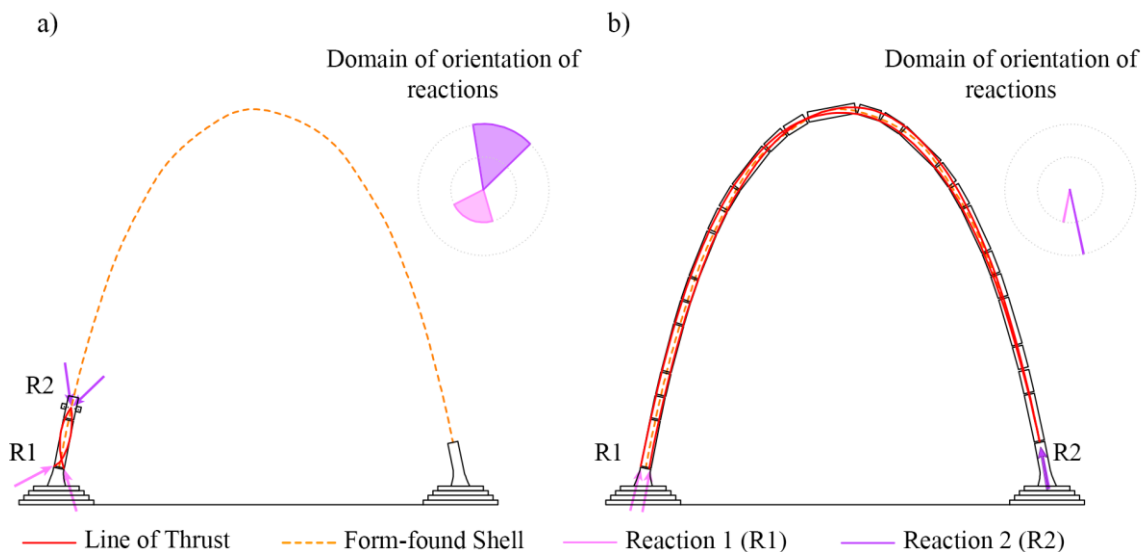


Figure 7. Domain of orientation of the reactions R1 and R2. a) First construction stage. b) Last construction stage of the central arch.

According to Heyman's theory [21], and due to the modest dimensions of the structure examined, geometrical instability is the most probable cause for collapse. Therefore, investigations on the variation of minimum and maximum lines of thrust during the construction works were carried out. As reported in Figure 7a), at the first stage of construction, with only two bricks positioned, a balanced state is found if the horizontal thrust comprised in the range of 0.00-0.001kN. Despite that, the domain of orientation of the reactions, denoted by R1 and R2, is wide: about 79.5° for R1, and 54.0° for R2. This domain expresses the number of possible safe solutions that can be found, i.e. the narrower it is, the fewer number of solutions are possible. With the progress of the construction works, see figure 7b), the minimum and maximum horizontal thrust increases, to 0.09-0.10 kN, while the domain of orientation of reactions drastically narrows down to, 1.1° for R1 and 0.8° for R2.

From a numerical point of view, the robotic arm's interaction with the structure was evaluated as a kinematic constraint: the gripping points of the robotic arms allow no displacement. The first numerical simulations showed that the equilibrium state is influenced by the position of the robotic gripping point,

highlighting that an incorrectly positioned grip could lead to out-of-plane displacement. Thus, as described in [34] [36], a particular robotic sequencing construction method has been developed in order to avoid out-of-plane twisting displacement. The simulation of the construction stages conducted with DEM confirms the results obtained by TLA: the central arch reaches an equilibrium state, with the robotic arm as support, in each construction stage of phase **I**. As shown in figure 8, the arch shows a **maximum displacement of $4.27 \cdot 10^{-3}$ mm**.

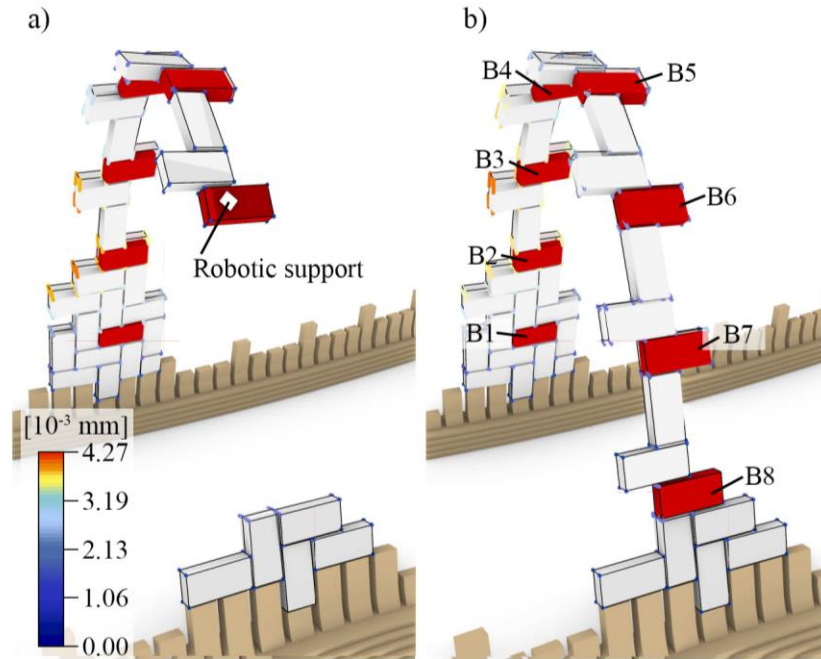


Figure 8. Construction stages of the central arch. a) incomplete arch showing the position of the robotic support. b) finished arch showing the position of control blocks (red) for the monitoring of displacements during the construction. The color scale is associated with the displacement vectors of each node.

5.2 Phase II

The structural behaviour of phase **II** has been investigated by DEM analysis. Here, the robotic arms work separately without supporting the shell during its construction, thus, the structure is required to reach a self-balanced state at each construction stage. The numerical analysis simulated the as-built construction process for the shell. Similar to phase **I**, the structural behaviour is investigated at each construction stage; the influence on the equilibrium is established as each brick is placed.

The analysis confirms the stability of the form-found shell; furthermore, as shown in figure 9, immediately after the completion of each of the construction stages **II-a**, **II-b**, **II-c** the magnitude of the displacement decreases. As the arch substructures are completed, it allows for a redistribution of the forces, consequently, improving the structural behaviour of the partially completed structure and reducing the overall displacements. Subsequently as the construction of the next part of the structure begins, the displacements again begin to increase. This phenomenon highlights the importance of the construction sequence and the masonry tessellation, inspired by the pitched vault and herringbone technique, respectively.

The surface illustrated in figure 9, denoted by ζ , shows the variation in the magnitude of the displacements in relation to the construction stages. The surface ζ is plotted based on monitoring the behaviour of eight control points: the centroids of the blocks B_i (B_1, B_2, \dots, B_8), shown in figure 8b. For example, referring to figure 9, the curve starting from B_1 in the centroid axis, expresses the variation of the magnitude of displacement recorded at the control point B_1 through each construction stage. The

surface ζ displays peaks and valleys orientated in the direction perpendicular to the construction stage axis, showing that as stages are completed the displacements decrease uniformly. The maximum displacement recorded is $4.6 \cdot 10^{-2}$ millimeters located near the intersection of the construction stage **II-c** and control point B_3 .

The surface ζ also describes the magnitude of the residual displacement of the completed final shell (**II-d**); at this construction stage the displacement seen is lower than the maximum displacements recorded during phases **II**. The reason for this decrease is that when the structure is completed, the geometry corresponds to the final form-found shell, for which the structural behaviour has been optimised.

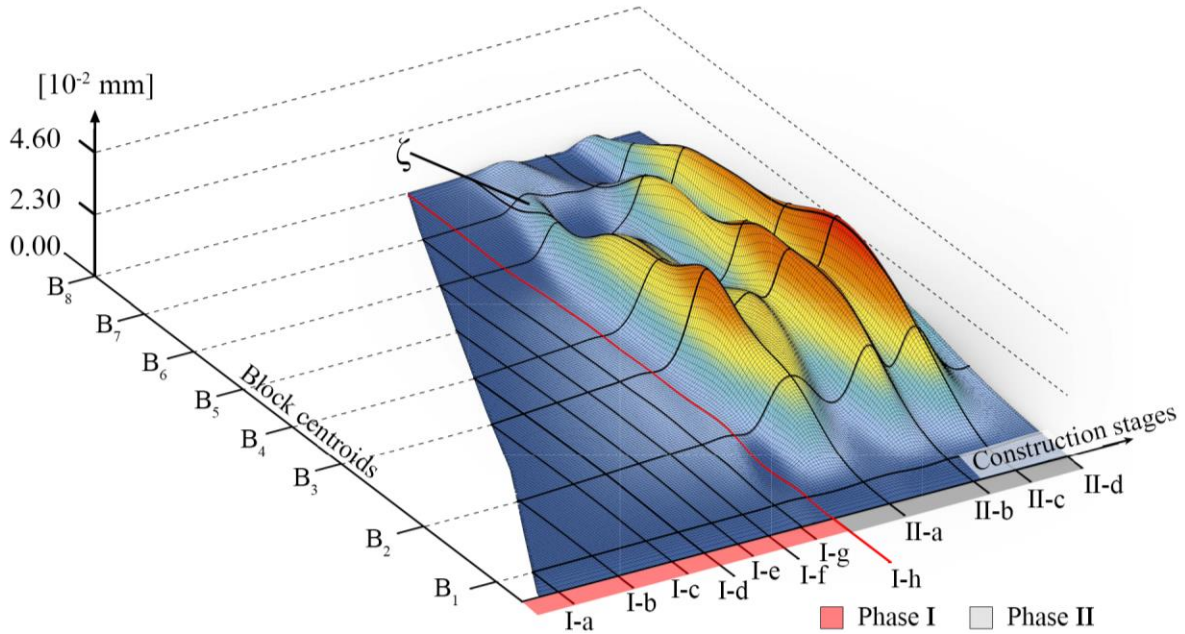


Figure 9. Displacement magnitudes surface (ζ). The vertical axis reports the magnitude of displacements. The other two axes represent the location of block centroids where the displacements have been recorded ($B_1, B_2, B_3, \dots, B_8$) and the construction stages divided by the two phases **I** and **II**. Here, **I-a, I-b, I-c, \dots, I-h** are subdivisions in phase **I**, while **II-a, II-b** and **II-c** are the construction stage as described in figure 4.

6. Conclusion

The potential of historical construction techniques, adopted in the context of emerging innovations in novel computational form-finding approaches and robotic construction technologies, is emphasised in the current case study. Similar to the construction of pitched vaults and herringbone vaults, factors such as, the construction process and masonry tessellation, assume primary relevance. These construction factors play a fundamental role in achieving an equilibrium state of the structure under construction. For example, in the current case, the presence of the central arch has a large influence on the stability of the construction works referenced as phase **II**, i.e., it supports the construction of the other portions of the vault, providing external reactions needed to reach an equilibrium state. Keeping this aim in mind, the knowledge of the structural state under construction is crucial; only through studies conducted in this manner can possible failures be identified. The analysis reported in sections 5.1 and 5.2 highlights the displacement and forces present in the structure under construction. TLA carried out at the end of the phase **I**, shows the existence of a narrow domain of orientation of support reactions, emphasizing that even if a balanced state could be found, a slight variation in the geometry of the arch or in the location and orientation of the supports, could lead to overturning or collapse of the shell.

Furthermore, the introduction of a temporal variable in the structural analysis allows mapping of variations in the structural behaviour throughout the construction process. As illustrated in section 5.2, the study of the surface ζ , shows the variation in the structural behaviour between phases **I** and **II**. In phase **I**, the balanced state can be reached only by arch behaviour, here, the surface ζ is regular and the maximum displacement recorded in the central arch is significantly lower than that of phase **II**, where the rest of the vault is constructed and a compressed membrane behavior occurs. In phase **II**, the surface ζ is described by peaks and valleys. Between the construction stage **I-h** and **II-a**, ζ shows a strong variation: the magnitude of displacement of all blocks of the central arch increases by an order, defining the first peak that corresponds to **II-a**. This temporal interval (between **I-h** and **II-a**) starts when the central arch is completed and ends when the substructure corresponding to the second arch is closed. Immediately after its completion (after **II-a**), a new and more stable structure exhibiting compression-shell behaviour occurs. With this altered structural behaviour, the magnitude of displacements decreases, which coincides with the first valley in ζ , as seen in figure 9. Further, the valleys correspond to construction stages which follow the completion of arch substructures, and where redistribution of forces occurs leading to a more stable shell behaviour. This phenomenon is even more evident at the completed vault stage (end of **II-d**), where the pure compression shell behaves as designed.

The paper originates from a study of the historical construction technologies. The analysis and the discussion reported here are extremely relevant to the field of contemporary self-balancing technologies and ultimately for the task of construction cost-optimisation. Only by considering the state of the structure during construction works, is it possible to assess the self-balanced state and thus, drastically decrease the material cost of construction [44]. Recent works [45] [46] have shown potential in this direction, using cooperative robotics and other non-traditional fabrication systems to build complex structures without formwork. These developments have the potential to impact the building industry, but first require a better framework for evaluating a structure's behaviour during all phases of construction. As research [17] also shows, this investigation is one of the first bricks placed along the path towards establishing such an analysis-framework.

Funding sources

The authors want to express their gratitude for providing 3DEC software under the Education Partnership Program. We would also like to acknowledge the Metropolis Project of Princeton University, and the Princeton Catalysis Initiative for financially supporting this project.

References

- [1] I. Papayianni, 'The longevity of old mortars', *Appl. Phys. A*, vol. 83, no. 4, pp. 685–688, Jun. 2006.
- [2] S. El-Naggar, 'Les voûtes dans l'architecture de l'Égypte ancienne', *Inst. Fr. Archéologie Orient.*, vol. 1, 1999.
- [3] G. w. Van Beek, 'Arches and Vaults in the Ancient Near East', *Sci. Am.*, vol. 257, no. 1, pp. 96–103, 1987.
- [4] R. Besenval, *Technologie de la voûte dans l'orient ancien*, vol. 1, 2 vols. Paris: Editions Recherche sur les civilisations, 1984.
- [5] P. Block, M. DeJong, L. Davis, and J. Ochsendorf, 'Tile vaulted systems for low-cost construction in Africa', vol. 7, no. 1, p. 10, 2010.
- [6] L. Davis, M. Rippmann, and T. Pawlofsky, 'Innovative funicular tile vaulting: A prototype vault in Switzerland', p. 12, 2012.
- [7] G. Conti, 'La spinapesce nel Rinascimento tra Filippo Brunelleschi, i Sangallo e Bernardo Buontale nella Grotta Grande del Giardino di Boboli : alcune considerazioni matematiche', *Spinapesce Nel Rinascim. Tra Filippo Brunelleschi Sangallo E Bernardo Buontale Nella Grotta*

- Gd. Giard. Boboli Alcune Considerazioni Mat.*, pp. 246–254, 2013.
- [8] S. Huerta, ‘The geometry and construction of Byzantine vaults: the fundamental contribution of Auguste Choisy’, in *Auguste Choisy (1841-1909). L’architecture et l’art de bâtir*, Madrid, Jan. 2009, pp. 289–305.
- [9] J. Ochsendorf, *Guastavino Vaulting: The Art of Structural Tile*. Princeton Architectural Press, 2014.
- [10] A. Fraddosio, N. Lepore, and M. D. Piccioni, ‘Further refinement of the Corbelling Theory for the equilibrium analysis of corbelled domes’, *Curved Layer. Struct.*, vol. 6, no. 1, pp. 30–40, Mar. 2019.
- [11] S. di Pasquale, P. L. Badini, and G. Tempesta, *Rappresentazione analitica e grafica della cupola di Santa Maria del Fiore*. Firenze: Cooperativa Libreria Universitatis Studii Fiorentini Via S. Gallo, 25 - Firenze, 1977.
- [12] A. Almagro, *Bóvedas tabicadas en la Cartuja de Granada: el final de un proceso evolutivo*. Universidad Politécnica de Valencia, 2012.
- [13] A. Pizzigoni, *Brunelleschi*, I. Bologna: Zanichelli, 1989.
- [14] A. Choisy, *Histoire de l’architecture.*, 1st ed., vol. 1, 2 vols. Paris: Gauthier-Villars, Imprimeur-Libraire du Bureau des Longitudes, de l’École Polytechnique, 1899.
- [15] F. Gurrieri, *La cupola del Brunelleschi*. Firenze: Accademia dell’Iris, 2010.
- [16] A. Pizzigoni, V. Paris, M. Pasta, M. Morandi, and A. Parsani, ‘Herringbone naked structure’, *Proc. IASS Annu. Symp.*, vol. 2018, no. 12, pp. 1–6, Jul. 2018.
- [17] V. Paris, A. Pizzigoni, and S. Adriaenssens, ‘Statics of self-balancing masonry domes constructed with a cross-herringbone spiraling pattern’, *Eng. Struct.*, vol. 215, p. 110440, Jul. 2020.
- [18] J. Ochsendorf, ‘Tile Vaulting Innovations by Rafael Guastavino Jr. and Eduardo Torroja’, *J. Int. Assoc. Shell Spat. Struct.*, vol. 61, no. 1, pp. 59–66, Mar. 2020.
- [19] D. L. López, T. V. Mele, and P. Block, ‘The combination of tile vaults with reinforcement and concrete’, *Int. J. Archit. Herit.*, vol. 13, no. 6, pp. 782–798, Aug. 2019.
- [20] J. Heyman, ‘On shell solutions for masonry domes’, *Int. J. Solids Struct.*, vol. 3, no. 2, pp. 227–241, Mar. 1967.
- [21] J. Heyman, ‘The stone skeleton’, *Int. J. Solids Struct.*, vol. 2, no. 2, pp. 249–279, Apr. 1966.
- [22] M. Angelillo, P. B. Lourenço, and G. Milani, ‘Masonry behaviour and modelling’, in *Mechanics of Masonry Structures*, M. Angelillo, Ed. Vienna: Springer, 2014, pp. 1–26.
- [23] P. Block, M. DeJong, and J. Ochsendorf, ‘As Hangs the Flexible Line: Equilibrium of Masonry Arches’, *Nexus Netw. J.*, vol. 8, no. 2, pp. 13–24, Oct. 2006.
- [24] L. Davis and P. Block, ‘Earthen Masonry Vaulting: Technologies and Technology Transfer’, in *Building Ethiopia: Sustainability and Innovation in Architecture and Design, Vol. I*, Ethiopian Institute of Architecture, Building Construction and City Development, 2012, pp. 219–233.
- [25] E. De Chiara, C. Cennamo, A. Gesualdo, A. Montanino, C. Olivieri, and A. Fortunato, ‘Automatic generation of statically admissible stress fields in masonry vaults’, *J. Mech. Mater. Struct.*, vol. 14, no. 5, pp. 719–737, Dec. 2019.
- [26] P. Block and J. Ochsendorf, ‘Thrust Network Analysis: A New Methodology for Three-Dimensional Equilibrium’, *J. Int. Assoc. Shell Spat. Struct.*, vol. 48, no. 3, pp. 167–173, Dec. 2007.
- [27] A. Fraddosio, N. Lepore, and M. D. Piccioni, ‘Thrust Surface Method: An innovative approach for the three-dimensional lower bound Limit Analysis of masonry vaults’, *Eng. Struct.*, vol. 202, p. 109846, Jan. 2020.
- [28] S. Vasilis, B. Katalin, L. V. José, and M. Gabriele, *Computational Modeling of Masonry Structures Using the Discrete Element Method*. IGI Global, 2016.
- [29] P. A. Cundall, ‘Formulation of a three-dimensional distinct element model—Part I. A scheme to detect and represent contacts in a system composed of many polyhedral blocks’, *Int. J. Rock*

- Mech. Min. Sci. Geomech. Abstr.*, vol. 25, no. 3, pp. 107–116, Jun. 1988.
- [30] R. Hart, P. A. Cundall, and J. Lemos, ‘Formulation of a three-dimensional distinct element model—Part II. Mechanical calculations for motion and interaction of a system composed of many polyhedral blocks’, *Int. J. Rock Mech. Min. Sci. Geomech. Abstr.*, vol. 25, no. 3, pp. 117–125, Jun. 1988.
- [31] D. L. Fang, R. K. Napolitano, T. L. Michiels, and S. M. Adriaenssens, ‘Assessing the stability of unreinforced masonry arches and vaults: a comparison of analytical and numerical strategies’, *Int. J. Archit. Herit.*, vol. 13, no. 5, pp. 648–662, Jul. 2019.
- [32] I. J. Oppenheim, D. J. Gunaratnam, and R. H. Allen, ‘Limit State Analysis of Masonry Domes’, *J. Struct. Eng.*, vol. 115, no. 4, pp. 868–882, Apr. 1989.
- [33] I. X. Han, E. P. G. Bruun, S. Marsh, M. Tavano, S. Adriaenssens, and S. Parascho, ‘From Concept to Construction: A Transferable Design and Robotic Fabrication Method for a Building-Scale Vault’, in *Proceedings of the 40th Annual Conference of the Association for Computer Aided Design in Architecture*, 2020, pp. 1–12. (To appear)
- [34] S. Parascho, I. X. Han, S. Walker, A. Beghini, E. P. G. Bruun, and S. Adriaenssens, ‘Robotic vault: a cooperative robotic assembly method for brick vault construction’, *Constr. Robot.*, vol. 4, no. 3, pp. 117–126, Dec. 2020.
- [35] S. Parascho, I. X. Han, A. Beghini, M. Mike, E. P. G. Bruun, and S. Adriaenssens, ‘LightVault: A Design and Robotic Fabrication Method for Complex Masonry Structures’, Paris (France), 2021. (To appear)
- [36] E. P. G. Bruun *et al.*, ‘Three Cooperative Robotic Fabrication Methods for the Scaffold-Free Construction of a Masonry Arch’, 2021, eprint: 2104.04856.
- [37] SOM, ‘Bricks, Mortar, and Robots: Solutions for Sustainable Construction’, *Medium*, Aug. 22, 2019. <https://som.medium.com/bricks-mortar-and-robots-solutions-for-sustainable-construction-f404b90fe9ab> (accessed Apr. 09, 2021).
- [38] M. Masaaki, I. Takeo, and B. Philippe, ‘Parametric Self-supporting Surfaces via Direct Computation of Airy Stress Functions’, *ACM Trans. Graph. TOG*, pp. 1–12, 2015.
- [39] M. Miki, E. Adiels, W. Baker, T. Mitchell, A. Sehlstrom, and C. Williams, ‘Form-Finding of Shells Containing Both Tension and Compression Using the Airy Stress Function’, Dec. 2020.
- [40] ‘Oatey, R Fix-It™ Stick Epoxy Putty’. 2020, [Online]. Available: URL <https://www.oatey.com/products/oatey-fixit-stick-epoxy-putty-1829259701>.
- [41] *3DEC | US Minneapolis - Itasca Consulting Group, Inc.* .
- [42] *Manual, Theory and Background*. Minneapolis: Itasca Consulting Group. Inc, 2016.
- [43] E. Çaktı, Ö. Saygılı, J. V. Lemos, and C. S. Oliveira, ‘Discrete element modeling of a scaled masonry structure and its validation’, *Eng. Struct.*, vol. 126, pp. 224–236, Nov. 2016
- [44] F. Barbosa *et al.*, ‘Reinventing Construction: A Route to Higher Productivity’, McKinsey Global Institute, 2017. Accessed: Mar. 25, 2021. [Online].
- [45] E. P. G. Bruun, I. Ting, S. Adriaenssens, and S. Parascho, ‘Human–robot collaboration: a fabrication framework for the sequential design and construction of unplanned spatial structures’, *Digit. Creat.*, pp. 1–17, Nov. 2020..
- [46] P. Latteur, S. Goessens, and C. Mueller, ‘Masonry construction with drones’, *Proc. IASS Annu. Symp.*, vol. 2016, no. 7, pp. 1–10, Sep. 2016.